







# Effective enhancement of the electron-phonon coupling driven by nonperturbative electronic density fluctuations

E. Moghadas<sup>a</sup> , M. Reitner<sup>a</sup> , T. Wehling<sup>b</sup> , G. Sangiovanni<sup>c</sup> , S. Ciuchi<sup>d</sup> , and A. Toschi<sup>a</sup> 

<sup>a</sup>*Institute of Solid State Physics, TU Wien, 1040 Vienna, Austria*

<sup>b</sup>*I. Institute for Theoretical Physics, Universität Hamburg, Notkestraße 9–11, 22607 Hamburg, Germany*

<sup>c</sup>*Institut für Theoretische Physik und Astrophysik und Würzburg-Dresden Cluster*

*of Excellence ct.qmat, Universität Würzburg, 97074 Würzburg, Germany and*

<sup>d</sup>*Dipartimento di Scienze Fisiche e Chimiche, Università dell'Aquila, Coppito-L'Aquila, Italy*

(Dated: March 18, 2025)

We present a dynamical mean-field study of the nonperturbative electronic mechanisms, which may lead to significant enhancements of the electron-phonon coupling in correlated electron systems. Analyzing the effects of electronic correlations on the lowest-order electron-phonon processes, we show that in the proximity of the Mott metal-to-insulator transition of the doped square lattice Hubbard model, where the isothermal charge response becomes particularly large at small momenta, the coupling of electrons to the lattice is strongly increased. This, in turn, induces significant corrections to both the electronic self-energy and phonon-mediated pairing interaction, indicating the possible onset of a strong interplay between lattice and electronic degrees of freedom even for small values of the bare electron-phonon coupling.

*Introduction.* The scattering processes of electrons and lattice vibrations (electron-phonon coupling) represent an important factor in determining thermodynamic and spectroscopic properties of condensed matter systems [1–3]. It is also widely known that these processes play a crucial role in the electronic pairing in conventional superconductors both at ambient [1, 2, 4, 5] and under high-pressure [6, 7]. In fact, an estimate of the magnitude of the electron-phonon coupling is often decisive [8] to classify the superconductivity shown by a given compound as “conventional” or “unconventional”, whereas the latter is typically driven by a purely electronic pairing mechanism. However, while the algorithmic progress of DFT-based methods in the last decades has allowed to reach an unprecedented level of precision for the quantitative estimates or the prediction of the electron-phonon coupling and their effects [6, 9], the corresponding treatment of this physics in strongly correlated electron systems [10–26] remains highly challenging.

In this paper, we address this longstanding problem from a fundamental perspective, (i) by performing a rigorous investigation of the renormalization of electron-phonon-coupling in the intermediate-to-strong coupling regime of electronic correlations and (ii) by evaluating the associated effects on the electron-electron pairing and on the electronic self-energy. In doing this, we also aim at clarifying the partially contradicting interpretations and results obtained by different groups in very early studies of this problem [12–14, 19], which were limited by the computational effort fifteen/twenty years ago.

In order to achieve these goals in the most basic framework, we have performed dynamical mean-field theory (DMFT) calculations, on both the one- and two-particle level, for the (hole-doped) Hubbard model [27, 28] in the close proximity of its Mott metal-to-insulator transition (MIT). The choice of DMFT allows an explicit treatment

of the non-perturbative effects of the electronic interaction [29–38], which –as we will demonstrate– play a pivotal role in the renormalization of the electron-phonon scattering. Further, the analytical insight recently gained on the momentum-dependent response function [35, 39, 40] of DMFT makes it possible to clarify the underlying origin of our numerical results, and of the emerging physics. Finally, we elaborate on the consequences and the limitations of our findings, as well as on the route they clearly suggest for future studies.

*Momentum-dependent charge response.* In our study we will focus on a typical realization of electron-phonon scattering, where the lattice vibrations are directly coupled to the electronic density. For this reason, we start by considering the (momentum-dependent) charge-response of the electronic system. This quantity describes, in general, the electronic density fluctuations, whereas in the static limit (i.e. with zero transfer frequency,  $\omega = 0$ , and vanishing transfer momentum  $\mathbf{q} \rightarrow 0$ ), yields the (electronic) isothermal compressibility,  $\kappa = \frac{1}{n^2} \partial n / \partial \mu = \frac{1}{n^2} \chi_{\mathbf{q} \rightarrow 0}(\omega = 0)$  [41–45],  $n$  being the electron density of the system and  $\mu$  its chemical potential.

As mentioned above, to investigate the effect of strong electronic correlations, we will exploit the DMFT applied to the hole-doped, single-band Hubbard model on the square lattice with unitary lattice spacing, on-site interaction  $U$ , and nearest neighboring hopping  $t$  (with  $4t = 1$ , i.e. with the half-bandwidth defining our energy units). In this respect, we recall that the pioneering DMFT works of Refs. [46–49] demonstrated that the electronic compressibility may become significantly enhanced in the vicinity of the critical endpoint of the Mott MIT. Specifically, this happens in slightly doped, as well as frustrated systems [50], where even a divergence of  $\kappa$  can be observed. At the same time, we should also note how the general understanding of the physical processes

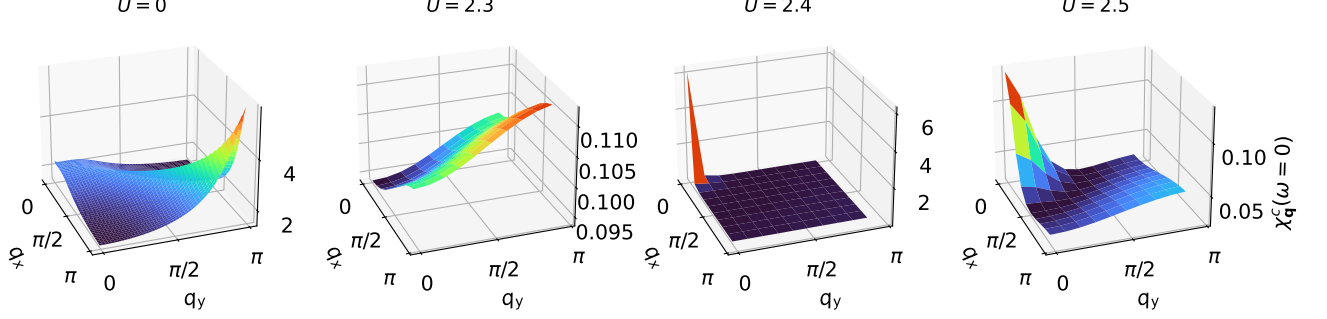


FIG. 1. Momentum dependence of the static charge susceptibility  $\chi_{\mathbf{q}}^c$  computed in DMFT for the 2D-Hubbard model on the square lattice for  $\beta = 55.75$  and  $n = 0.9966$  at the bosonic frequency  $\omega = 0$  and evaluated for varying  $U$  values.

controlling this phenomenon has recently advanced by means of the combined analytical/numerical studies in Refs. [35, 39, 40, 51]. In particular, these studies identified the purely non-perturbative mechanisms controlling the significant enhancement of the uniform charge response in parameter regimes, where the on-site charge fluctuations get significantly suppressed by the strong electronic interaction.

Based on these considerations, we extend the derivation of Refs.[35, 40], obtaining the following spectral representation, which yields a rather precise description of the momentum-dependent charge susceptibility of DMFT for the square lattice in the intermediate-to-strong-coupling regime:

$$\chi_{\mathbf{q}}^c(\omega=0) \equiv \chi_{\mathbf{q}}^c \simeq \sum_{\alpha} \left( \lambda_{\alpha}^{-1} + \frac{1}{2}\beta \mathcal{T}_{\mathbf{q}} \right)^{-1} w_{\alpha} \quad (1)$$

Here,  $\lambda_{\alpha}$  denotes the eigenvalues of the generalized on-site static charge susceptibility of the system,  $\chi_{loc}^{\nu\nu'\omega=0}$ , expressed as a matrix in the fermionic Matsubara frequency space  $\{\nu, \nu'\}$ , while its associated eigenvectors  $V_{\alpha}^{\nu}$  yield the spectral weight  $w_{\alpha} = [\sum_{\nu} V_{\alpha}^{-1}(\nu)] \times [\sum_{\nu'} V_{\alpha}(\nu')]$ . The momentum dependence of Eq. (1) is enclosed in the quantity  $\beta^2 \left( [\chi_{0,\mathbf{q}}^{\nu\nu'}]^{-1} - [\chi_{0,loc}^{\nu\nu'}]^{-1} \right) \approx 2t^2 [\cos(q_x) + \cos(q_y)] \delta_{\nu\nu'} = \mathcal{T}_{\mathbf{q}} \delta_{\nu\nu'}$  (see [52]), where the fermionic Matsubara frequencies are defined as  $\nu = (2n+1)\pi/\beta$ ,  $\forall n \in \mathbb{Z}$  and  $\chi_{0,\mathbf{q}}^{\nu\nu'} = -\beta \sum_{\mathbf{k}} G_{\mathbf{k}}^{\nu} G_{\mathbf{k}+\mathbf{q}}^{\nu'} \delta_{\nu\nu'}$  denotes the DMFT dressed bubble, with  $G_{\mathbf{k}}^{\nu}$  being the DMFT Green's function and  $\chi_{0,loc}^{\nu\nu'} = \sum_{\mathbf{q}} \chi_{0,\mathbf{q}}^{\nu\nu'}$  its local counterpart. We note that this expression, albeit approximate, generalizes the exact one which can be defined for the bipartite Bethe lattice with infinite coordination at  $\mathbf{q} = 0$  and  $\mathbf{q} = (\pi, \pi, \pi, \dots)$ .

While Eq. (1) will be quite useful for interpreting the numerical results presented below, as well as starting point for additional derivations, it immediately allows to define the condition for a strong enhancement of  $\chi_{\mathbf{q}}^c$ , namely when  $\lambda_{\alpha}^{-1} \rightarrow -\frac{1}{2}\beta \mathcal{T}_{\mathbf{q}}$  [35]. In particular, accord-

ing to Eq. (1) the divergence of the electronic compressibility, would occur when the lowest eigenvalue of the on-site generalized charge susceptibility  $\lambda_I$  becomes negative enough to fulfill the condition  $\lambda_I^{-1} \rightarrow -\frac{1}{2}\beta \mathcal{T}_{\mathbf{q}=0} \approx -\beta t^2 < 0$ . This is evidently possible only after a sign-flip of  $\lambda_I$  (which is typically positive at weak-coupling) occurs, which features a *non-invertibility* of the Bethe-Salpeter equations for the on-site charge susceptibility [29, 30, 32–34, 37, 53–56] and marks a breakdown of the corresponding self-consistent perturbation expansion [31, 33, 38, 57, 58]. Eventually, as the decreasing values of the eigenvalues  $\lambda_{\alpha}$  with  $U$  can be, to some extent, associated to the freezing of the on-site charge fluctuations, induced by the pre-formation of local magnetic moments [36, 38, 54, 59, 60], Eq. (1) also directly clarifies [35] how a substantial increase of the  $\mathbf{q} = 0$  charge response of the system can be driven, in the non-perturbative regime, by a suppression of the on-site charge fluctuations.

*Numerical results.* We now turn to our numerical DMFT investigation regarding the evolution of the charge susceptibility as a function of the interaction  $U$ . Specifically, we consider here the case of a slightly hole-doped (i.e.  $n = 0.9966$ ) Hubbard model at  $\beta = 55.75$ , which allow us, by varying  $U$ , to be in the close proximity of the corresponding critical endpoint of the half-filled Mott MIT. In Fig. 1, we present the full momentum dependence of the charge susceptibility for different values of  $U$ . We note, that in the non-interacting  $U = 0$  case (leftmost panel), the charge response is dominated by the contribution of the  $\mathbf{q} = (\pi, \pi)$  sector, due to the perfect nesting properties of the square lattice [61] considered. Upon turning the interaction up to  $U = 2.3$  (second panel), one observes, as generally expected on the basis of perturbation theory arguments (cf. RPA), a gradual, overall suppression of the charge susceptibility at all momenta. In particular, the predominance of larger transfer momenta is still retained, in spite of a much weaker  $\mathbf{q}$ -dependence. The situation changes drastically once the interaction value of  $U = 2.4$  (corresponding to a parameter set very close to the half-filled MIT) is reached (third

panel), where a strong enhancement for the isothermal susceptibility occurs: A sharp peak around  $\mathbf{q} = (0, 0)$  emerges, signaling the tendency towards a phase separation instability. For larger  $U$  values (rightmost panel), further proceeding into the bad-metallic region, we continue to observe the peak at low transfer momenta, although with a smaller overall magnitude. The drastic difference in the momentum structure between the metallic ( $U < 2.4$ ) and the bad-metallic ( $U \geq 2.4$ ) regime can be quantitatively understood in terms of the spectral representation of the charge response introduced in Eq. (1). Specifically, as explicitly illustrated in [52], the spectral weight  $w_I$ , associated to the lowest eigenvalue  $\lambda_I$  (responsible for the emergence of the  $\mathbf{q} = (0, 0)$  peak [62]), is vanishingly small in the whole weak-coupling/metallic regime. It obtains, however, a sizable value in the bad-metallic regime, determining the sudden change in the momentum dependence of the numerically calculated  $\chi_{\mathbf{q}}^c$  we observe at  $U = 2.4$ .

Further, in the whole bad-metallic regime the explicit expression of Eq. (1), with  $\mathcal{T}_{\mathbf{q}} \approx 2t^2 [\cos(q_x) + \cos(q_y)]$  works as an excellent approximation, allowing to derive an analytic expression for the momentum structure of the charge response. For small transfer momenta, one gets  $\mathcal{T}_{\mathbf{q}} \approx 2t^2 + \epsilon \mathbf{q}^2 + \mathcal{O}(\mathbf{q}^4)$ , which yields the following explicit expression for the physical charge susceptibility as (for details see [52]):

$$\chi_{\mathbf{q}}^c = \sum_{\alpha} \frac{\chi_{\alpha} w_{\alpha}}{1 + (\xi_{\alpha} \mathbf{q})^2} \quad (2)$$

where  $\chi_{\alpha} = \left( \lambda_{\alpha}^{-1} + \frac{t^2}{2\beta} \right)^{-1}$  and  $\xi_{\alpha}^2 = \epsilon \chi_{\alpha}$ . Evidently, this expression is highly reminiscent of an Ornstein-Zernike (OZ) function [63–65], which represents, in fact, a reliable parametrization for the isothermal charge compressibility computed in DMFT, in the vicinity of its second-order phase transition [66]. In particular, by recasting Eq. (2) in an explicit OZ form (i.e.,  $[\chi_{\mathbf{q}}^c]^{-1} \sim \mathbf{q}^2 + \xi^{-2}$  [67]) the corresponding correlation length  $\xi$  can be explicitly expressed in terms of the eigenvalues of the local susceptibility [52]

$$\xi^2 \cong \frac{\sum_{\alpha} \xi_{\alpha}^2 \chi_{\alpha} w_{\alpha}}{\sum_{\alpha} \chi_{\alpha} w_{\alpha}} \quad (3)$$

which in the subsequent section will turn out to be a useful relation for the analysis of the renormalization effects of the electron-phonon coupling.

*Effect on the electron-phonon vertex.* After the above discussion on the nonperturbative enhancement of the electronic charge susceptibility, it is natural to pose the question how/to what extent this phenomenon can manifest itself in the renormalization of the electron-phonon (el-ph) coupling. To this end, we consider the most simple case of optical Holstein phonons with a characteristic frequency of  $\omega_0$  and extend the Hubbard Hamiltonian by

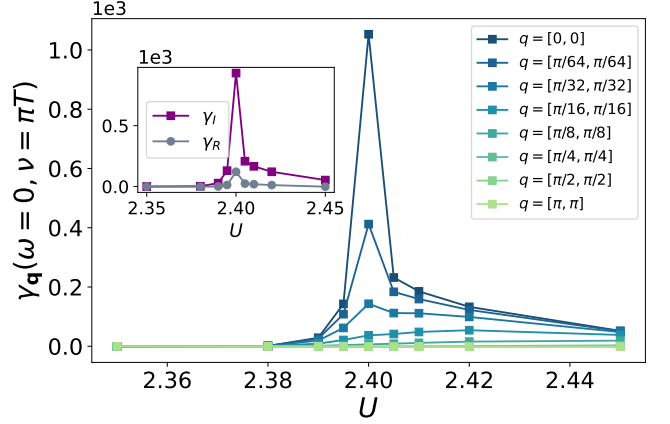


FIG. 2. Renormalized electron phonon vertex  $\gamma_{\mathbf{q}} = \tilde{g}_{\mathbf{q}}/g_0$  extracted from  $\chi_{\mathbf{q}}^c$  as a function of  $U$  at the lowest bosonic/fermionic frequencies at  $\beta = 55.75$ . Inset: Contribution of the lowest eigenvalue to  $\gamma_{\mathbf{q}}$  ( $\gamma_I$ ), in comparison to the contribution of the remaining eigenvalues ( $\gamma_R$ ).

an additional interaction term with the bare, local coupling  $g_0$  defined as  $\mathcal{H}_{el-ph} = g_0 \sum_{\mathbf{k}, \mathbf{q}} c_{\mathbf{k}+\mathbf{q}}^\dagger c_{\mathbf{k}} (b_{\mathbf{q}} + b_{-\mathbf{q}}^\dagger)$  where  $b$  ( $b^\dagger$ ) denote the bosonic annihilation (creation) operators. In the spirit of Refs. [12–14, 19] we consider corrections to the el-ph vertex linear in the bare  $g_0$ . Hence, the renormalized coupling  $\tilde{g}$  will contain purely electronic interactions. Diagrammatically, we can define this renormalized el-ph vertex function, through the following dimensionless expression, as

$$\gamma_{\mathbf{q}}^\nu = \tilde{g}_{\mathbf{q}}/g_0 = \left[ \chi_{0,\mathbf{q}}^\nu \right]^{-1} \sum_{\nu'} \chi_{\mathbf{q}}^{c,\nu\nu'}, \quad (4)$$

where we omitted the  $\delta_{\nu\nu'}$  term of the bubble for the sake of brevity. Extending the analytical results of Ref. [35] and of the previous section, it is straightforward to show that the renormalized el-ph vertex can be expressed in terms of the on-site generalized susceptibility's eigenbasis via

$$\gamma_{\mathbf{q}}^\nu = \sum_{\alpha} \left( \lambda_{\alpha}^{-1} + \frac{1}{2} \beta \mathcal{T}_{\mathbf{q}} \right)^{-1} \tilde{w}_{\alpha}^\nu \quad (5)$$

where  $\tilde{w}_{\alpha}^\nu = \beta^2 (\chi_{0,\mathbf{q}}^\nu)^{-1} V_{\alpha}(\nu) \sum_{\nu'} V_{\alpha}^{-1}(\nu')$ . This highlights the purely *non-perturbative* connection between the enhancement of the  $\mathbf{q} = 0$  charge response and the el-ph coupling. In fact, both quantities share the same divergence condition ( $\lambda_I^{-1} \rightarrow -\frac{1}{2} \beta \mathcal{T}_{\mathbf{q}=0} \approx -\beta t^2 < 0$ ), whereas the spectral weight for the renormalized vertex is slightly modified. The DMFT results for  $\gamma_{\mathbf{q}}^\nu$  evaluated at the lowest fermionic frequency  $\nu = \pi T$ , obtained for the same parameter values as the charge susceptibility, are shown in Fig. 2. On the basis of Eq. (5), it is clear that the aforementioned momentum differentiation between the weakly-correlated/metallic and the bad metallic regimes previously discussed for the charge susceptibility gets also directly reflected onto the behavior

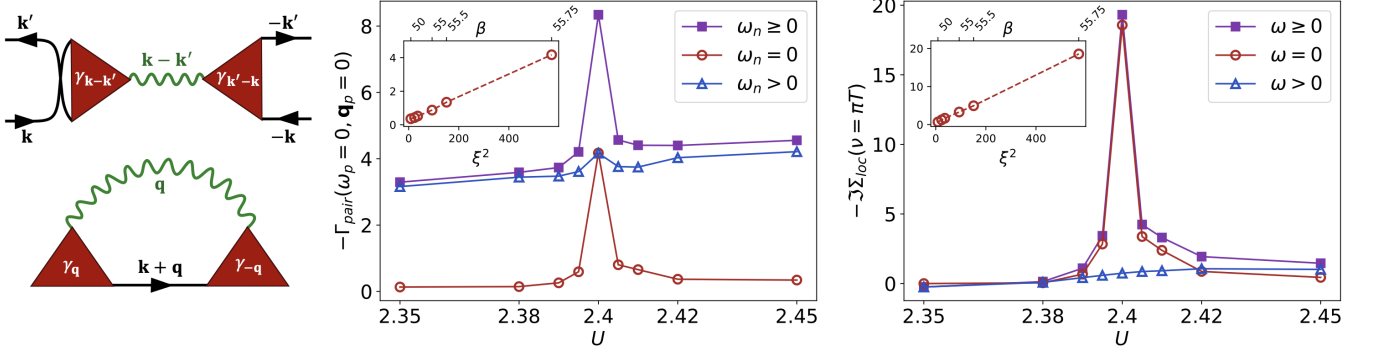


FIG. 3. Left panel: Lowest order contributions in  $g_0$  to the phonon-mediated pairing interaction and to the electronic self-energy. Central panel:  $U$ -dependence of the pairing diagram (violet)  $\beta = 55.75$ , split in its contributions arising from the zero (red) and finite frequency (blue) contributions. Inset: Dependence of the zero-frequency contribution to the pairing diagram on the correlation length and inverse temperature. Right panel: Same plots as for the central panel, but for the self-energy corrections (s. text).

of  $\gamma_{\mathbf{q}}^{\nu}$ . Specifically, for  $U < 2.4$ , an extremely reduced renormalized el-ph coupling, which is strongly suppressed  $\gamma_{\mathbf{q}}^{\nu=\pi T} \ll 1$  and essentially independent of the transfer momentum, is found, consistent with the conventional, gradual suppression of the charge response by increasing interactions. However, by further increasing the interaction up to  $U \cong 2.4$ , the renormalized el-ph vertex suddenly exhibits a huge enhancement at low transfer momenta  $\mathbf{q}$ . This reaches its maximum at  $U = 2.4$  and then slowly decreases with growing interaction values. Consistent with our previous discussions, we observe that this enhancement is largely dominated by the behavior of the lowest, real eigenvalue  $\lambda_I$  of the impurity susceptibility, which almost fulfills the divergence criterion at  $U = 2.4$  (for details cf. [52]). In the inset of Fig. 2 we compare the contribution of  $\lambda_I$  to the renormalized vertex, here denoted by  $\gamma_I$ , with the contribution of the remaining eigenvalues and show that the observed enhancement predominantly arises from the lowest eigenvalue. At the same time, while the behavior of  $\gamma_{\mathbf{q}}^{\nu=\pi T}$  in this regime is evidently controlled by the underlying evolution of  $\chi_{\mathbf{q}}^c$ , we observe nonetheless a relative enhancement of the renormalized el-ph coupling (w.r.t. the non-interacting case, where  $\gamma_{\mathbf{q}}^{\nu=\pi T} \equiv 1$ ) which is larger by *two orders of magnitude* than for the corresponding charge response. This additional enhancement can be ascribed to the prefactor proportional to the inverse dressed DMFT bubble term in Eq. (5), as  $\chi_{0,\mathbf{q}}^{\nu}$  gets strongly suppressed at low-frequencies in the bad-metallic regime. This extra factor might have caused some contradicting interpretations in the past literature, as in the region of small but finite  $\mathbf{q}$ , the enhancement of  $\gamma_{\mathbf{q}}^{\nu=\pi T}$  can become numerically visible, even *before* the corresponding increasing of  $\chi_{\mathbf{q}}^c$  [52]. In any case, the overall similarity between  $\gamma_{\mathbf{q}}^{\nu}$  and  $\chi_{\mathbf{q}}^c$  and in the proximity of the Mott MIT suggest that the former may also display a OZ-like momentum structure. Indeed in [52], we demonstrate that this expectation holds, by explicitly deriving such an OZ expression as well as the

associated correlation length: We get the same formulae as in Eqs. (2)-(3) with the sole substitution of  $w_{\alpha} \rightarrow \tilde{w}_{\alpha}$ . It is worth noticing, that in a first approximation, close to the MIT, where the physical behaviors are dominated by the contribution of the lowest eigenvalue  $\lambda_I$ , the correlation lengths associated with the OZ expressions for  $\gamma_{\mathbf{q}}^{\nu=\pi T}$  and  $\chi_{\mathbf{q}}^c$  will become equivalent [52].

*Renormalization of the electronic quantities.* After addressing the effect of enhanced charge fluctuations on the el-ph coupling, we turn to analyze the role this strong renormalization plays on the electronic system. To this end, we start by considering the effective electron-electron pairing interaction mediated by the exchange of one single phonon taking the aforementioned vertex renormalization effects into account. The corresponding pairing diagram, depicted in the upper left panel of Fig. 3, can be thus viewed as a *perturbative* correction to the electronic scattering in the pairing up to *second order* in the bare el-ph coupling. This may provide a reasonable starting point for analyzing the regime of small bare el-ph coupling in the presence of strong electronic correlation ( $g_0 \ll U$ ).

For zero transfer energy and momentum in the pairing channel (i.e.  $\omega_p = 0, \mathbf{q}_p = 0$ ) this interaction reads

$$\Gamma_{pair} = \frac{g_0^2}{\beta^2} \sum_{\nu\nu'} \int d^2k d^2k' \gamma_{\mathbf{k}-\mathbf{k}'}^{\nu,-\nu'} D_0^{\nu-\nu'} \gamma_{\mathbf{k}'-\mathbf{k}}^{\nu',-\nu} \quad (6)$$

where  $D_0^{\omega} = \frac{-2\omega_0}{\omega_n^2 + \omega_0^2}$  denotes the bare Holstein-phonon propagator. Using an OZ parametrization, i.e.  $\gamma_{\mathbf{q}} \propto \xi^2 [1 + (\xi\mathbf{q})^2]^{-1}$ , and performing a change of variables corresponding to  $\mathbf{q} = \mathbf{k} - \mathbf{k}'$  allows us to rewrite the above as

$$\Gamma_{pair} = \frac{g_0^2}{\beta^2} \sum_{\nu\omega} \int d^2q \gamma_{-\mathbf{q}}^{\nu,-\omega} D_0^{\omega} \gamma_{\mathbf{q}}^{\nu\omega} \quad (7)$$

$$\cong \frac{-2g_0^2}{\omega_0 \beta^2} \sum_{\nu} \int d^2q \frac{\gamma_{\mathbf{q}=0}^{\nu} \gamma_{\mathbf{q}=0}^{-\nu}}{[1 + (\xi\mathbf{q})^2]^2} + \sum_{\omega>0} \mathcal{R}(\omega) \quad (8)$$



where  $\mathcal{R}(\omega)$  is a regular function of the positive bosonic Matsubara frequencies, i.e.  $\omega_n = 2n * \pi/\beta, \forall n \in \mathbb{N}^*$ . A quick glance at the momentum integral immediately reveals an infrared singularity. This yields a divergence of  $\Gamma_{pair}$  that, in 2D, scales with the square of the correlation length  $\xi$  [68]. In the central panel of Fig. 3, we show then our numerical data for  $\Gamma_{pair}$ , evaluated using Eq. (7) as a function of  $U$  and decompose it into the contributions arising from the static ( $\omega = 0$ ) and dynamic ( $\omega > 0$ ) components. We clearly observe the effect of the static contribution to the overall behavior of  $\Gamma_{pair}$ , namely a prominent peak at the critical interaction value of  $U = 2.4$  in contrast to a rather weak- $U$  dependence of the ( $\omega > 0$ ) terms [69]. Moreover, we can analyze the dependence of  $\Gamma_{pair}$  on the correlation length by evaluating its (strongly enhanced) static contribution for different values of  $\beta$  (s. inset of Fig. 3, central panel). As expected from the momentum structure of the (approximated) Eq. (8), the numerical evaluation of this quantity reveals a quadratic dependence on  $\xi$ .

Among the several Feynman diagrams, entailing second-order corrections in  $g_0$  to the DMFT (purely electronic) self-energy, which display the leading contributing in  $\xi$  in the proximity of the phase-separation instability [70], we focus on the one depicted in the lower left panel of Fig. 3, which was often considered in previous works [20, 21, 71, 72] and which displays an evident diagrammatic similarity to the pairing interaction process discussed above. By following essentially the same step as for the calculations of  $\Gamma_{pair}$ , we get:

$$\Delta\Sigma_{\mathbf{k}}^{\nu} = \frac{g_0^2}{\beta} \sum_{\omega} \int d^2q \gamma_{-\mathbf{q}}^{\nu,-\omega} G_{\mathbf{k}+\mathbf{q}}^{\nu+\omega} D_0^{\omega} \gamma_{\mathbf{q}}^{\nu\omega} \quad (9)$$

$$\cong \frac{-2g_0^2}{\omega_0 \beta} \int d^2q \frac{G_{\mathbf{k}+\mathbf{q}}^{\nu} (\gamma_{\mathbf{q}=0}^{\nu})^2}{[1 + (\xi\mathbf{q})^2]^2} + \sum_{\omega>0} \mathcal{R}(\omega) \quad (10)$$

Due to the weak  $\mathbf{k}$ -dependence of the Green's function in the strongly correlated regime, the 2D integral will result, similar as for  $\Gamma_{pair}$ , in a  $\xi^2$ -dependence. These considerations are confirmed by our numerical evaluation of Eq. (9) reported in the right panel of Fig. 3. In particular, for the sake of conciseness, we plot the local corrections to the DMFT self-energy (i.e.  $\int d^2k \Delta\Sigma_{\mathbf{k}}^{\nu}$ ) as a function of  $U$  as well as, in the inset, its static contribution as a function of  $\beta$ . The former data set indicates a huge enhancement of the el-ph corrections to the DMFT self-energy, while the latter confirms the expected  $\xi^2$  scaling in the proximity of the non-perturbative phase-separation instability of the electronic system. We emphasize here, that in all previous considerations it is, in fact, the *elastic* part of the el-ph scattering to be enhanced due the electronic correlations. Phonons will thus behave as classical scatterers irrespective of their quantum nature.

**Conclusions.** Our analysis demonstrates how a huge renormalization of a weak bare el-ph coupling may be actually triggered by enhanced small- $\mathbf{q}$  charge-fluctuations

in the proximity of a Mott MIT. This is in contrast to the generically expected suppression of the el-ph coupling due to the suppression of charge fluctuations and a loss of spectral weight at the fermi surface. Such a non-perturbative phenomenon directly reverberates into a corresponding increase of the effective pairing interaction, with possibly relevant consequences for multiorbital/Hund's metal systems [10, 41, 73–79], where phase-separation instabilities are found in larger portions of their DMFT phase-diagrams [40, 80, 81]. At the same time, the equally large magnitude of the estimated self-energy corrections indicates, for large  $\xi$ , the breakdown of the second-order diagrammatic approach adopted in our study, calling for future self-consistent investigations of the Hubbard-Holstein-physics [16–18, 22, 82–84] based, e.g., on diagrammatic extensions of DMFT [85].

**Acknowledgements.** We thank Aiman Al Eryani, Sabine Andergassen, Massimo Capone, Emmanuele Cappelluti, Sergio Caprara, Herbert Ebl, Samuele Giuli and Alexander Kowalski for useful discussions. E.M., M.R. and A.T. acknowledge support from the Austrian Science Fund (FWF) through the grant 10.55776/I5868 (Project P1 of the research unit QUAST, for5249, of the German Research Foundation, DFG). M.R. further acknowledges support as a recipient of a DOC fellowship of the Austrian Academy of Sciences. G.S. and T.W. acknowledge support from the DFG through FOR 5249-449872909 (Project P05). S.C. acknowledges funding from NextGenerationEU National Innovation Ecosystem grant ECS00000041 - VITALITY - CUP E13C22001060006 and grant PE00000023 - IEXSMA - CUP E63C22002180006. At this point we also want to thank the WWAQ-organization for their hospitality. Calculations have been performed on the Vienna Scientific Cluster (VSC).

- 
- [1] A. A. Abrikosov, L. P. Gorkov, and I. E. Dzyaloshinski, *Methods of quantum field theory in statistical physics* (Courier Corporation, 2012).
  - [2] G. Rickayzen, *Green's Functions and Condensed Matter*, Dover Books on Physics (Dover Publications, Incorporated, 2013).
  - [3] G. D. Mahan, *Many-particle physics* (Springer Sci:(ence & Business Media, 2013).
  - [4] M. Tinkham, *Introduction to Superconductivity*, 2nd ed. (Dover Publications, Mineola, NY, 2004).
  - [5] P.-G. de Gennes, *Superconductivity of Metals and Alloys*, revised edition ed. (Westview Press, Boulder, CO, 1999).
  - [6] J. A. Flores-Livas, L. Boeri, A. Sanna, G. Profeta, R. Arita, and M. Eremets, A perspective on conventional high-temperature superconductors at high pressure: Methods and materials, *Physics Reports* **856**, 1 (2020), a perspective on conventional high-temperature superconductors at high pressure: Methods and materials.

- [7] M. I. Eremets, V. S. Minkov, A. P. Drozdov, and P. P. Kong, The characterization of superconductivity under high pressure, *Nature Materials* **23**, 26 (2024).
- [8] L. Boeri, O. V. Dolgov, and A. A. Golubov, Is  $\text{LaFeAsO}_{1-x}\text{F}_x$  an electron-phonon superconductor?, *Phys. Rev. Lett.* **101**, 026403 (2008).
- [9] F. Giustino, Electron-phonon interactions from first principles, *Rev. Mod. Phys.* **89**, 015003 (2017).
- [10] M. Grilli and C. Castellani, Electron-phonon interactions in the presence of strong correlations, *Phys. Rev. B* **50**, 16880 (1994).
- [11] L. Pietronero, S. Strässler, and C. Grimaldi, Nonadiabatic superconductivity. i. vertex corrections for the electron-phonon interactions, *Phys. Rev. B* **52**, 10516 (1995).
- [12] Z. Huang, W. Hanke, E. Arrigoni, and D. Scalapino, Electron-phonon vertex in the two-dimensional one-band hubbard model, *Physical Review B* **68**, 220507 (2003).
- [13] E. Koch and R. Zeyher, Renormalization of the electron-phonon coupling in the one-band hubbard model, *Phys. Rev. B* **70**, 094510 (2004).
- [14] E. Cappelluti, B. Cerruti, and L. Pietronero, Charge fluctuations and electron-phonon interaction in the finite- $u$  hubbard model, *Phys. Rev. B* **69**, 161101 (2004).
- [15] O. Rösch and O. Gunnarsson, Apparent electron-phonon interaction in strongly correlated systems, *Phys. Rev. Lett.* **93**, 237001 (2004).
- [16] G. Sangiovanni, M. Capone, C. Castellani, and M. Grilli, Electron-phonon interaction close to a mott transition, *Phys. Rev. Lett.* **94**, 026401 (2005).
- [17] G. Sangiovanni, O. Gunnarsson, E. Koch, C. Castellani, and M. Capone, Electron-phonon interaction and antiferromagnetic correlations, *Phys. Rev. Lett.* **97**, 046404 (2006).
- [18] G. Sangiovanni, M. Capone, and C. Castellani, Relevance of phonon dynamics in strongly correlated systems coupled to phonons: Dynamical mean-field theory analysis, *Phys. Rev. B* **73**, 165123 (2006).
- [19] A. Di Ciolo, J. Lorenzana, M. Grilli, and G. Seibold, Charge instabilities and electron-phonon interaction in the hubbard-holstein model, *Phys. Rev. B* **79**, 085101 (2009).
- [20] O. Rösch, G. Sangiovanni, and O. Gunnarsson, Sum rules and vertex corrections for electron-phonon interactions, *Phys. Rev. B* **75**, 035119 (2007).
- [21] O. Gunnarsson and O. Rösch, Interplay between electron-phonon and coulomb interactions in cuprates, *Journal of Physics: Condensed Matter* **20**, 043201 (2008).
- [22] M. Capone, C. Castellani, and M. Grilli, Electron-phonon interaction in strongly correlated systems, *Advances in Condensed Matter Physics* **2010**, 920860 (2010).
- [23] Z. Chen, Y. Wang, S. N. Rebec, T. Jia, M. Hashimoto, D. Lu, B. Moritz, R. G. Moore, T. P. Devereaux, and Z.-X. Shen, Anomalous strong near-neighbor attraction in doped 1d cuprate chains, *Science* **373**, 1235 (2021).
- [24] Y. Wang, Z. Chen, T. Shi, B. Moritz, Z.-X. Shen, and T. P. Devereaux, Phonon-mediated long-range attractive interaction in one-dimensional cuprates, *Phys. Rev. Lett.* **127**, 197003 (2021).
- [25] M. Jiang, Enhancing  $d$ -wave superconductivity with nearest-neighbor attraction in the extended hubbard model, *Phys. Rev. B* **105**, 024510 (2022).
- [26] Z. Shen, J. Liu, H.-X. Wang, and Y. Wang, Signatures of the attractive interaction in spin spectra of one-dimensional cuprate chains, *Phys. Rev. Res.* **6**, L032068 (2024).
- [27] J. Hubbard, Electron correlations in narrow energy bands, *Proc. R. Soc. Lond. A* **276**, 238 (1963).
- [28] M. Qin, T. Schäfer, S. Andergassen, P. Corboz, and E. Gull, The hubbard model: A computational perspective, *Annual Review of Condensed Matter Physics* **13**, 275 (2022), <https://doi.org/10.1146/annurev-conmatphys-090921-033948>.
- [29] T. Schäfer, G. Rohringer, O. Gunnarsson, S. Ciuchi, G. Sangiovanni, and A. Toschi, Divergent precursors of the mott-hubbard transition at the two-particle level, *Phys. Rev. Lett.* **110**, 246405 (2013).
- [30] T. Schäfer, S. Ciuchi, M. Wallerberger, P. Thunström, O. Gunnarsson, G. Sangiovanni, G. Rohringer, and A. Toschi, Nonperturbative landscape of the mott-hubbard transition: Multiple divergence lines around the critical endpoint, *Phys. Rev. B* **94**, 235108 (2016).
- [31] O. Gunnarsson, G. Rohringer, T. Schäfer, G. Sangiovanni, and A. Toschi, Breakdown of traditional many-body theories for correlated electrons, *Phys. Rev. Lett.* **119**, 056402 (2017).
- [32] P. Chalupa, P. Gunacker, T. Schäfer, K. Held, and A. Toschi, Divergences of the irreducible vertex functions in correlated metallic systems: Insights from the anderson impurity model, *Phys. Rev. B* **97**, 245136 (2018).
- [33] J. Vučković, N. Wentzell, M. Ferrero, and O. Parcollet, Practical consequences of the luttinger-ward functional multivaluedness for cluster dmft methods, *Phys. Rev. B* **97**, 125141 (2018).
- [34] D. Springer, P. Chalupa, S. Ciuchi, G. Sangiovanni, and A. Toschi, Interplay between local response and vertex divergences in many-fermion systems with on-site attraction, *Phys. Rev. B* **101**, 155148 (2020).
- [35] M. Reitner, P. Chalupa, L. Del Re, D. Springer, S. Ciuchi, G. Sangiovanni, and A. Toschi, Attractive effect of a strong electronic repulsion: The physics of vertex divergences, *Phys. Rev. Lett.* **125**, 196403 (2020).
- [36] P. Chalupa, T. Schäfer, M. Reitner, D. Springer, S. Andergassen, and A. Toschi, Fingerprints of the local moment formation and its kondo screening in the generalized susceptibilities of many-electron problems, *Phys. Rev. Lett.* **126**, 056403 (2021).
- [37] M. Pelz, S. Adler, M. Reitner, and A. Toschi, Highly nonperturbative nature of the mott metal-insulator transition: Two-particle vertex divergences in the coexistence region, *Phys. Rev. B* **108**, 155101 (2023).
- [38] S. Adler, F. Krien, P. Chalupa-Gantner, G. Sangiovanni, and A. Toschi, Non-perturbative intertwining between spin and charge correlations: A “smoking gun” single-boson-exchange result, *SciPost Phys.* **16**, 054 (2024).
- [39] M. Reitner, L. Crippa, D. R. Fus, J. C. Budich, A. Toschi, and G. Sangiovanni, Protection of correlation-induced phase instabilities by exceptional susceptibilities, *Phys. Rev. Res.* **6**, L022031 (2024).
- [40] A. Kowalski, M. Reitner, L. Del Re, M. Chatziefthymiou, A. Amaricci, A. Toschi, L. de’ Medici, G. Sangiovanni, and T. Schäfer, Thermodynamic stability at the two-particle level, *Phys. Rev. Lett.* **133**, 066502 (2024).
- [41] C. Watzenböck, M. Edelmann, D. Springer, G. Sangiovanni, and A. Toschi, Characteristic Timescales of the Local Moment Dynamics in Hund’s metals, *Phys. Rev. Lett.* **125**, 086402 (2020).
- [42] R. M. Wilcox, Bounds for the isothermal, adiabatic, and

- isolated static susceptibility tensors, *Phys. Rev.* **174**, 624 (1968).
- [43] F. Krien, E. G. C. P. van Loon, H. Hafermann, J. Otsuki, M. I. Katsnelson, and A. I. Lichtenstein, Conservation in two-particle self-consistent extensions of dynamical mean-field theory, *Phys. Rev. B* **96**, 075155 (2017).
- [44] F. Krien, E. G. C. P. van Loon, M. I. Katsnelson, A. I. Lichtenstein, and M. Capone, Two-particle fermi liquid parameters at the mott transition: Vertex divergences, landau parameters, and incoherent response in dynamical mean-field theory, *Phys. Rev. B* **99**, 245128 (2019).
- [45] E. G. C. P. van Loon, H. Hafermann, A. I. Lichtenstein, and M. I. Katsnelson, Thermodynamic consistency of the charge response in dynamical mean-field based approaches, *Phys. Rev. B* **92**, 085106 (2015).
- [46] G. Kotliar, S. Murthy, and M. J. Rozenberg, Compressibility divergence and the finite temperature mott transition, *Phys. Rev. Lett.* **89**, 046401 (2002).
- [47] P. Werner and A. J. Millis, Doping-driven mott transition in the one-band hubbard model, *Phys. Rev. B* **75**, 085108 (2007).
- [48] M. Eckstein, M. Kollar, M. Potthoff, and D. Vollhardt, Phase separation in the particle-hole asymmetric hubbard model, *Phys. Rev. B* **75**, 125103 (2007).
- [49] R. Nourafkan, M. Côté, and A.-M. S. Tremblay, Charge fluctuations in lightly hole-doped cuprates: Effect of vertex corrections, *Phys. Rev. B* **99**, 035161 (2019).
- [50] G. Kotliar, S. Murthy, and M. J. Rozenberg, Compressibility divergence and the finite temperature mott transition, *Phys. Rev. Lett.* **89**, 046401 (2002).
- [51] E. G. C. P. van Loon, F. Krien, and A. A. Katanin, Bethe-salpeter equation at the critical end point of the mott transition, *Phys. Rev. Lett.* **125**, 136402 (2020).
- [52] See Supplemental Material available under [URL] for details on xyz. This also includes Refs. xxx..
- [53] V. Janiš and V. Pokorný, Critical metal-insulator transition and divergence in a two-particle irreducible vertex in disordered and interacting electron systems, *Phys. Rev. B* **90**, 045143 (2014).
- [54] O. Gunnarsson, T. Schäfer, J. P. F. LeBlanc, J. Merino, G. Sangiovanni, G. Rohringer, and A. Toschi, Parquet decomposition calculations of the electronic self-energy, *Phys. Rev. B* **93**, 245102 (2016).
- [55] P. Thunström, O. Gunnarsson, S. Ciuchi, and G. Rohringer, Analytical investigation of singularities in two-particle irreducible vertex functions of the hubbard atom, *Phys. Rev. B* **98**, 235107 (2018).
- [56] H. Eßl, M. Reitner, G. Sangiovanni, and A. Toschi, General shiba mapping for on-site four-point correlation functions, *Phys. Rev. Res.* **6**, 033061 (2024).
- [57] E. Kozik, M. Ferrero, and A. Georges, Nonexistence of the luttinger-ward functional and misleading convergence of skeleton diagrammatic series for hubbard-like models, *Phys. Rev. Lett.* **114**, 156402 (2015).
- [58] H. Eßl, M. Reitner, E. Kozik, and A. Toschi, [How to stay on the physical branch in self-consistent many-electron approaches](#) (2025), [arXiv:2502.01420 \[cond-mat.str-el\]](#).
- [59] T. B. Mazitov and A. A. Katanin, Local magnetic moment formation and kondo screening in the half-filled single-band hubbard model, *Phys. Rev. B* **105**, L081111 (2022).
- [60] T. B. Mazitov and A. A. Katanin, Effect of local magnetic moments on spectral properties and resistivity near interaction- and doping-induced mott transitions, *Phys. Rev. B* **106**, 205148 (2022).
- [61] A. Georges, G. Kotliar, W. Krauth, and M. J. Rozenberg, Dynamical mean-field theory of strongly correlated fermion systems and the limit of infinite dimensions, *Rev. Mod. Phys.* **68**, 13 (1996).
- [62] M. Reitner, *Generalized Susceptibilities of the Anderson Impurity Model: Fingerprints of Local Moment Physics and Kondo Screening at the Two-Particle Level*, Project work, Technischen Universität Wien (2019).
- [63] L. Ornstein and F. Zernike, The influence of accidental deviations of density on the equation of state, *Koninklijke Nederlandsche Akademie van Wetenschappen Proceedings* **19**, 1312 (1914).
- [64] T. Moriya, *Spin fluctuations in itinerant electron magnetism*, Springer series in solid-state sciences, Vol. 56 (Springer, Berlin, 1985).
- [65] N. Goldenfeld, *Lectures On Phase Transitions And The Renormalization Group*, Frontiers in physics (Westview Press, 1992).
- [66] It is important to emphasize here, that, different from, e.g., antiferromagnetic phase-transitions, the phase-separation instability relevant for our study belongs to the Ising universality class. Hence, it will not be necessarily destroyed by spatial fluctuations beyond DMFT even in the 2D system considered.
- [67] Rigorously speaking, one would expect the OZ momentum dependence of  $[\chi_q^c]^{-1}$  to be corrected as  $|\mathbf{q}|^{2-\eta}$ ,  $\eta = \frac{1}{4}$  being the corresponding anomalous exponent of the 2D Ising class [86].
- [68] Note that even the explicit inclusion of the anomalous exponent  $\eta$  in the OZ expression would not prevent such a divergence, which would occur with a slightly modified scaling,  $\sim \xi^{\frac{3}{2}}$ .
- [69] This difference is due to the purely static nature of  $\chi_{\mathbf{q}=0}^c(\omega)$ , which directly reflects the conservation of the total electric charge in the system.
- [70] A more detailed discussion of the different class of elph diagrams, and their scaling behavior in  $\xi$ , based on a rather general treatment à la ab-initio DFA [87] can be found in [52].
- [71] A. Rubtsov, M. Katsnelson, and A. Lichtenstein, Dual boson approach to collective excitations in correlated fermionic systems, *Annals of Physics* **327**, 1320 (2012).
- [72] E. G. C. P. van Loon, A. I. Lichtenstein, M. I. Katsnelson, O. Parcollet, and H. Hafermann, Beyond extended dynamical mean-field theory: Dual boson approach to the two-dimensional extended hubbard model, *Phys. Rev. B* **90**, 235135 (2014).
- [73] M. Grilli, R. Raimondi, C. Castellani, C. Di Castro, and G. Kotliar, Phase separation and superconductivity in the  $u=\infty$  limit of the extended multiband hubbard model, *International Journal of Modern Physics B* **05**, 309 (1991), <https://doi.org/10.1142/S0217979291000195>.
- [74] K. Haule and G. Kotliar, Coherence-incoherence crossover in the normal state of iron oxypnictides and importance of hund's rule coupling, *New Journal of Physics* **11**, 025021 (2009).
- [75] L. de' Medici, J. Mravlje, and A. Georges, Janus-faced influence of hund's rule coupling in strongly correlated materials, *Phys. Rev. Lett.* **107**, 256401 (2011).
- [76] S. Mandal, R. E. Cohen, and K. Haule, Strong pressure-dependent electron-phonon coupling in fese, *Phys. Rev.*

- B **89**, 220502 (2014).
- [77] L. de' Medici, Hund's induced fermi-liquid instabilities and enhanced quasiparticle interactions, *Phys. Rev. Lett.* **118**, 167003 (2017).
  - [78] P. Villar Arribi and L. de' Medici, Hund-enhanced electronic compressibility in fese and its correlation with  $T_c$ , *Phys. Rev. Lett.* **121**, 197001 (2018).
  - [79] A. Isidori, M. Berović, L. Fanfarillo, L. de' Medici, M. Fabrizio, and M. Capone, Charge disproportionation, mixed valence, and janus effect in multiorbital systems: A tale of two insulators, *Phys. Rev. Lett.* **122**, 186401 (2019).
  - [80] M. Chatziefleftheriou, A. Kowalski, M. Berović, A. Amaricci, M. Capone, L. De Leo, G. Sangiovanni, and L. de' Medici, Mott quantum critical points at finite doping, *Phys. Rev. Lett.* **130**, 066401 (2023).
  - [81] A. Georges, L. d. Medici, and J. Mravlje, Strong correlations from hund's coupling, *Annual Review of Condensed Matter Physics* **4**, 137 (2013).
  - [82] E. Berger, P. Valášek, and W. von der Linden, Two-dimensional hubbard-holstein model, *Phys. Rev. B* **52**, 4806 (1995).
  - [83] A. Macridin, B. Moritz, M. Jarrell, and T. Maier, Synergistic polaron formation in the hubbard-holstein model at small doping, *Phys. Rev. Lett.* **97**, 056402 (2006).
  - [84] N. C. Costa, K. Seki, S. Yunoki, and S. Sorella, Phase diagram of the two-dimensional hubbard-holstein model, *Communications Physics* **3**, 80 (2020).
  - [85] G. Rohringer, H. Hafermann, A. Toschi, A. A. Katanin, A. E. Antipov, M. I. Katsnelson, A. I. Lichtenstein, A. N. Rubtsov, and K. Held, Diagrammatic routes to nonlocal correlations beyond dynamical mean field theory, *Rev. Mod. Phys.* **90**, 025003 (2018).
  - [86] K. Huang, *Statistical Mechanics*, 2nd ed. (John Wiley & Sons, New York, 1987).
  - [87] A. Toschi, G. Rohringer, A. Katanin, and K. Held, Ab initio calculations with the dynamical vertex approximation, *Annalen der Physik* **523**, 698 (2011).